



Field Induced Quantum Critical Point in YbAgGe

Sergey L. Bud'ko

and

Paul C. Canfield

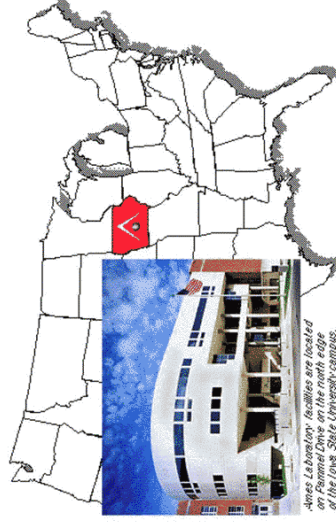
Ames Laboratory US DOE,
Department of Physics and Astronomy,
Iowa State University

canfield@ameslab.gov and budko@ameslab.gov

Supported by the Director for Energy Research, Office of Basic Energy Sciences, US DOE



Ames Laboratory



Mid-sized DOE Laboratory with ~ 400 employees
Organized in 1947 as a part of Manhattan Project

Now:

Applied Mathematics and Computational Sciences
Chemical and Biological Sciences

Condensed Matter Physics

Environmental and Protection Sciences

Granular and Multiphase Systems

Materials Chemistry

Materials and Engineering Physics

Non-Destructive Evaluation

Also:

Biorenewable Resources Consortium

Materials Preparation Center

Iowa State University

Large Land Grant University

~25,000 Students

**Known for Ag. (not Silver), Vet.,
and, in our circles, Physics and
Chemistry associated with
Ames Lab.**



In collaboration with:

Emilia Morosan, Yuri Janssen, Yuriy Mozharivskiy, Stephanie Law (ISU);

Björn Fåk (CEA/Grenoble), Desmond McMorrow (Univ. College /London);
Philipp Niklowitz, Jacques Flouquet (CEA/Grenoble)

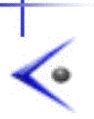
Discussions with:

Jörg Schmalian, Maxim Dzero (ISU) **and I hope many of you here at the workshop.**

Also thanks to:



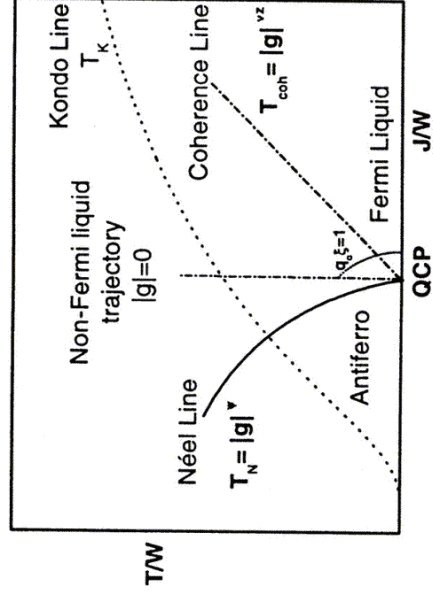
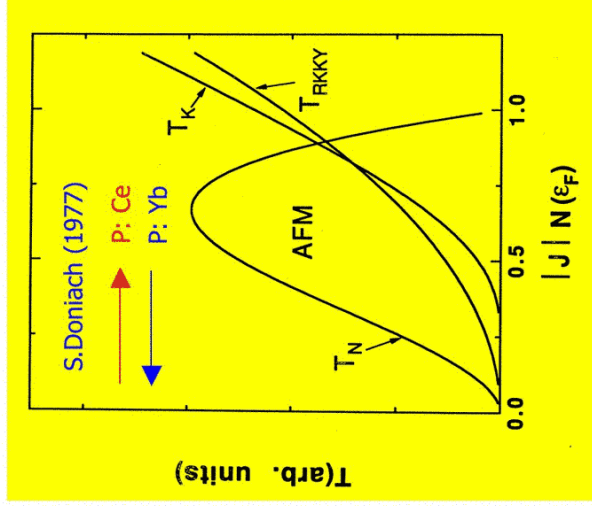
and A. Paul Ness, Marc D. McGinn (ISU)



Outline and salient papers

- Thermodynamic and Transport Properties of RAgGe (R = Tb – Lu) single crystals, E. Morosan et al., JMMM 277 (2004) 298. (cond-mat/0309327)
- Angular-dependent planar metamagnetism in the hexagonal compounds TbPtIn and TmAgGe, E. Morosan et al., PRB 71 (2005) xxxx. (cond-mat/0408121)
- Magnetic field induced non-Fermi-liquid behavior in YbAgGe single crystals, S. L. Bud'ko et al., PRB 69 (2004) 014415. (cond-mat./0308517)
- Hall effect in single crystal heavy Fermion YbAgGe, S. L. Bud'ko et al., PRB 71 (2005) xxxx. (cond-mat./0406435)
- Inelastic neutron scattering study of single crystal heavy fermion YbAgGe, B. Fak et al., J. Phys. Cond. Matter 17 (2005) 301
- Low temperature transport properties of YbAgGe near a quantum critical point, P. Niklowitz et al., unpublished.

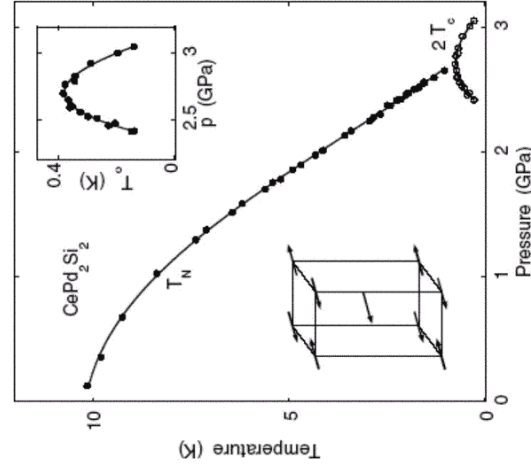
Doniach's phase diagram and QCP



Usually pressure or substitution

M. Continentino (1989) and many others before and mostly after...

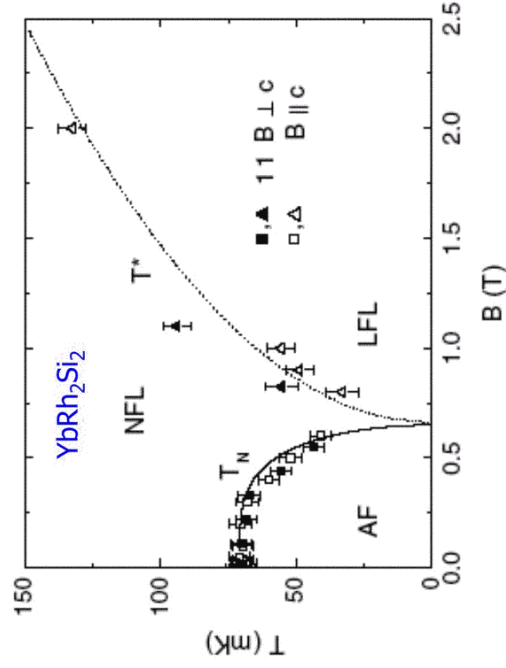
QCP – experimental examples (P, x, H)



Grosche et al., JPCM 13 (2001) 2845

(Similar results for CeIn₃)

pressure



Gegenwart et al., PRL 89 (2002) 056402.

applied field



QCP – experimental examples

Problems: **substitution** \Rightarrow disorder
pressure: discontinuity, difficult

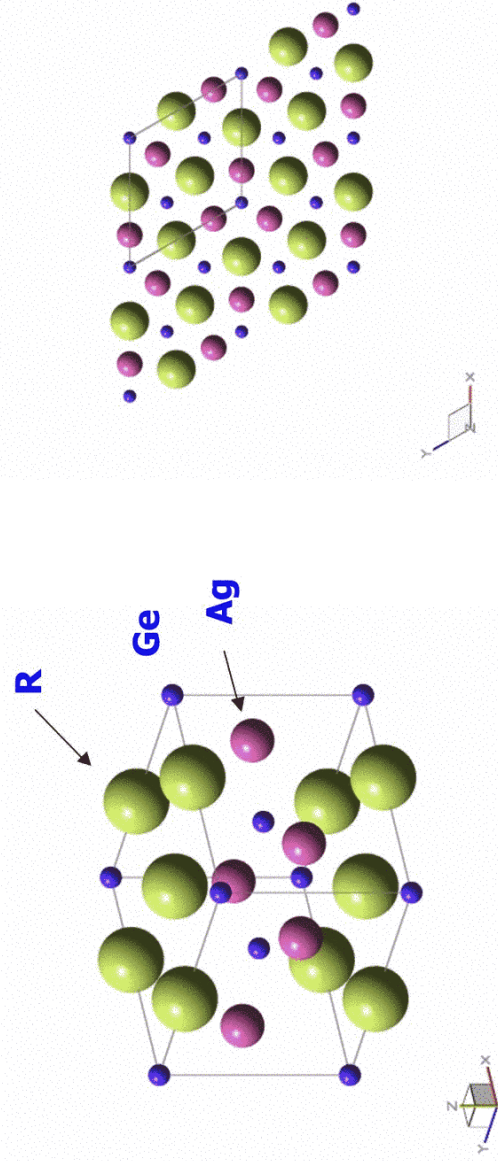
Magnetic field: continuous, more measurements are accessible.

Are P, x, H “equivalent”? Is there any single, “universal” picture?

More, “clean” examples needed!



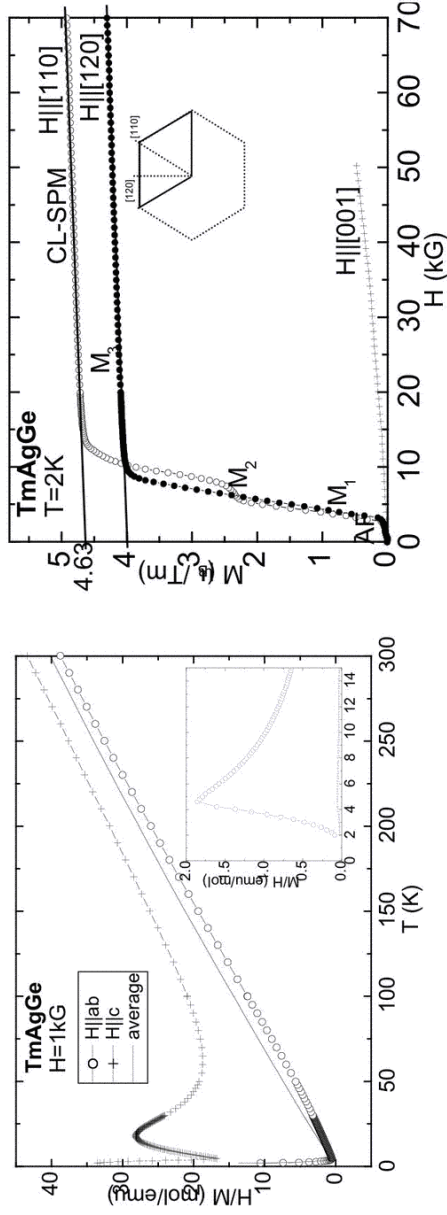
RAgGe - structure



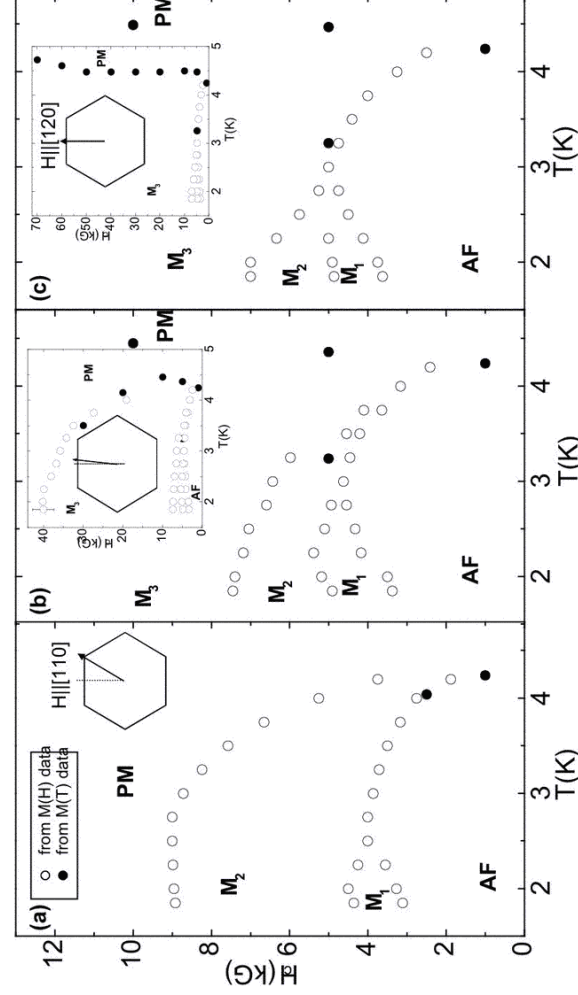
Hexagonal P-62m, R in orthorhombic point symmetry
 For RAgGe overview see E.Morosan et al. JMMM 277 (2004) 298.
 Lots of curious stuff: metamagnetism, “unconventional” resistivity, etc. for R = Tb-Tm.

- "Thermodynamic and transport properties of RAgGe (R = Tb - Lu) single crystals", E. Morosan *et al.*, J. Magn. Magn. Mater. **277** (2004) 298 and cond-mat/0309327
- "Angular dependent planar metamagnetism in the hexagonal compounds TbPtIn and TmAgGe", E. Morosan *et al.*, Phys. Rev. B (in press) and cond-mat/0408121.

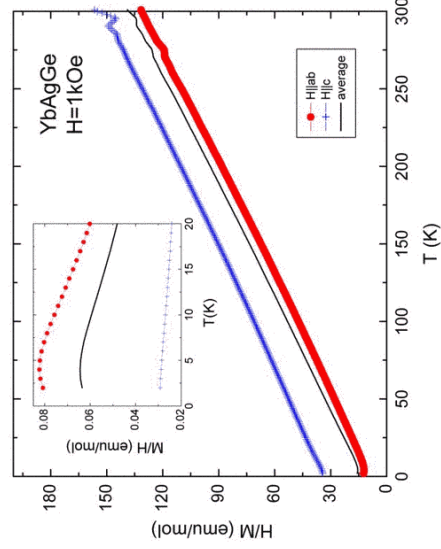
TmAgGe:



TmAgGe:

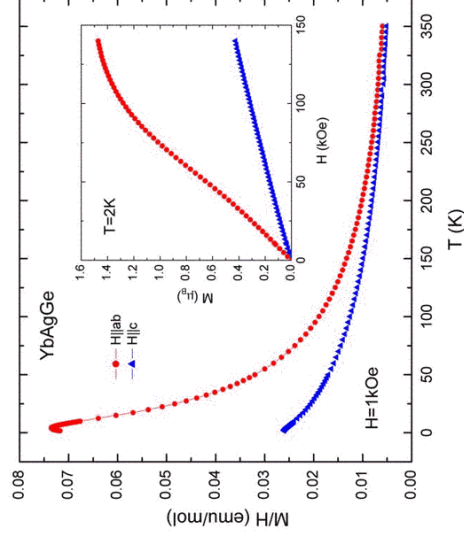


YbAgGe – basic properties



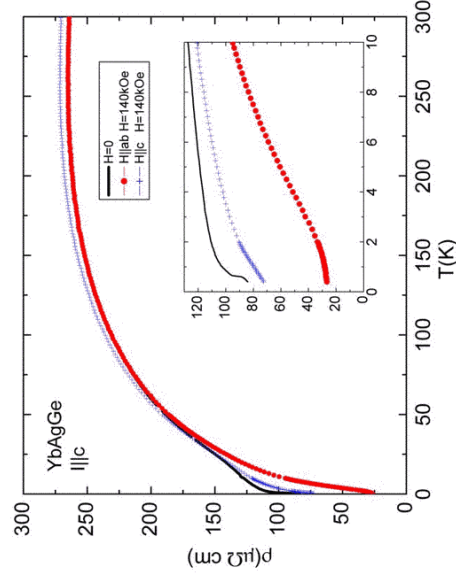
$$\Theta_{ave} \approx -30 \text{ K}$$

Deviations from CW law in χ_{ave} below $\sim 20 \text{ K}$



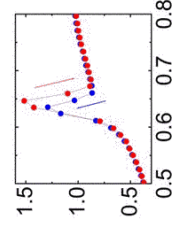
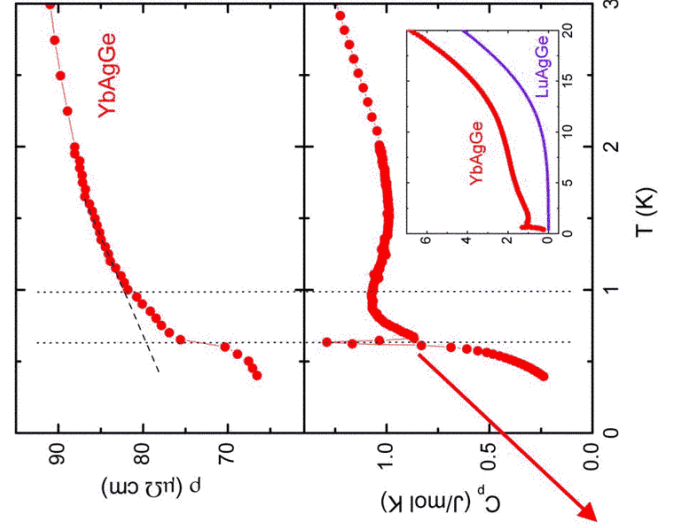
E.Morosan et al., JMMM 277 (2004) 298

YbAgGe – basic properties

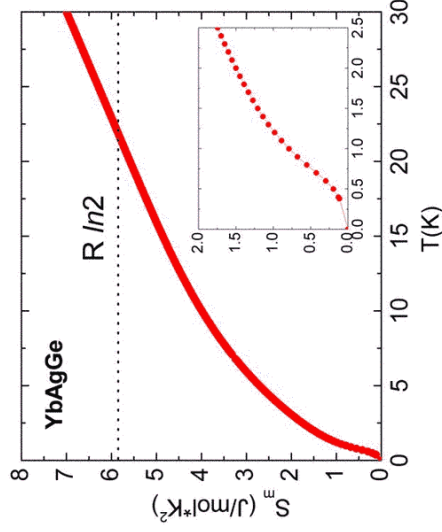
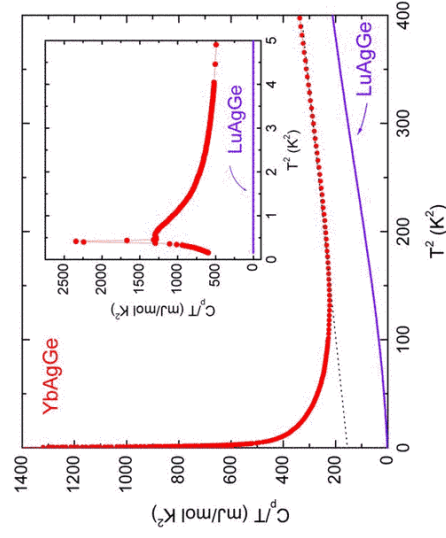


$$T_M \approx 0.65\text{K}, 1\text{K}$$

E.Morosan et al., JMMM 277 (2004) 298; SLB et al., PRB 69 (2004) 014415



YbAgGe – basic properties



$\gamma \approx 150 \text{ mJ/mol K}^2$ from 10K-20K range extrapolation. More realistic estimate: $150 \text{ mJ/mol K}^2 \leq \gamma \leq 1\text{J/mol K}^2$

- (i) YbAgGe is new Yb-based HF (or close to being HF)
- (ii) LRO below 1K, probably small moment ordering

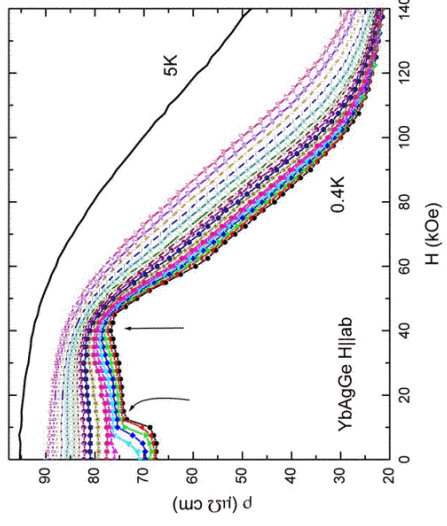
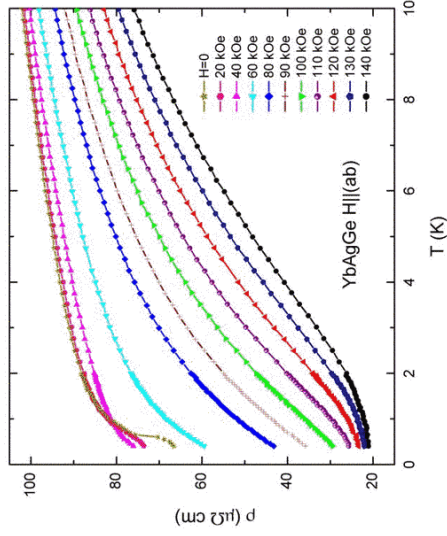
⇒ **good candidate for suppression of T_N to QCP**



YbAgGe – estimate of some parameters

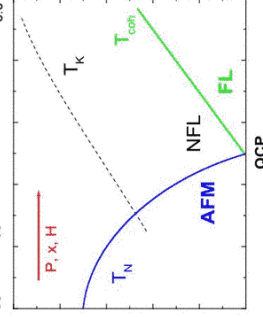
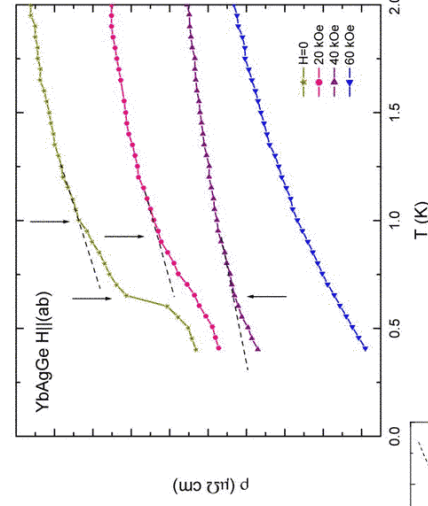
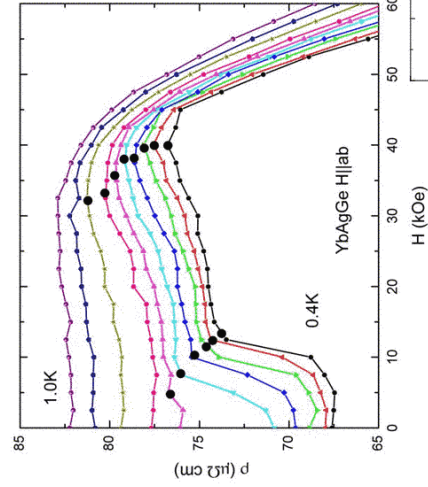
- ◆ **$150 \text{ mJ/mol K}^2 \leq \gamma \leq 1\text{J/mol K}^2$**
- ◆ **$\Theta_{\text{ave}} \approx -30 \text{ K}$, $\Theta/10 \leq T_K \leq \Theta \Rightarrow 3\text{K} \leq T_K \leq 30 \text{ K}$**
- ◆ **$T_K = w_N \pi^3 R / 6\gamma$**
 $w_N = 0.4107$ (Wilson number), R – gas constant \Rightarrow **$15\text{K} \leq T_K \leq 120 \text{ K}$**
- ◆ **Wilson ratio: $R = 4\chi\pi^2 k_B^2 / 3\gamma\mu_{\text{eff}}^2 \approx 1.8$**
 ($R = 1$ for non-interacting electrons, $R = 2$ for heavy fermions)

YbAgGe – resistivity in applied field

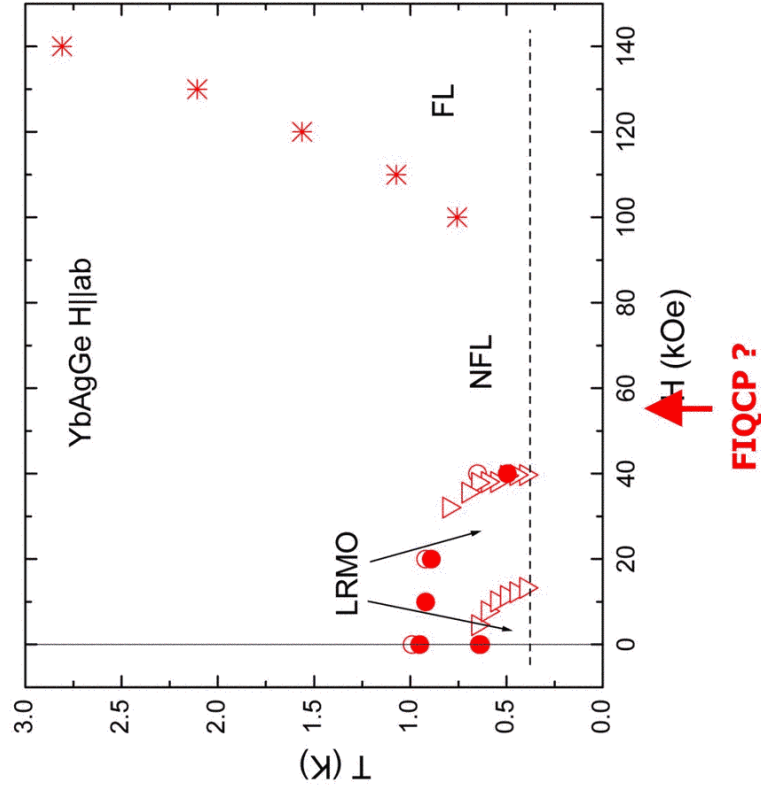


Let us look in more detail

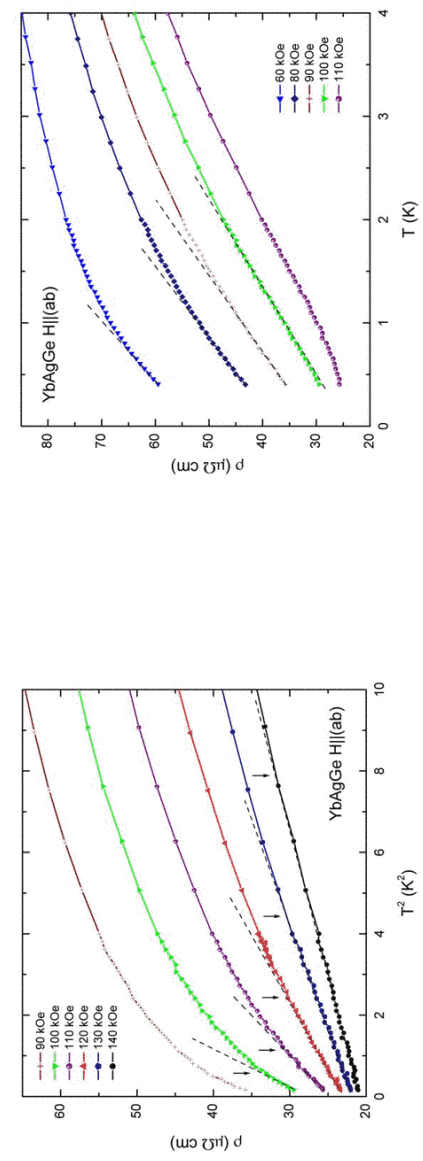
YbAgGe - $\rho(T,H)$: shift of magnetic transitions in applied field



YbAgGe – phase diagrams

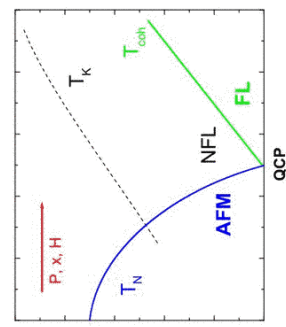


YbAgGe - $\rho(T,H)$: Fermi-liquid vs. non-Fermi-liquid

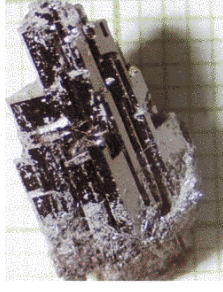
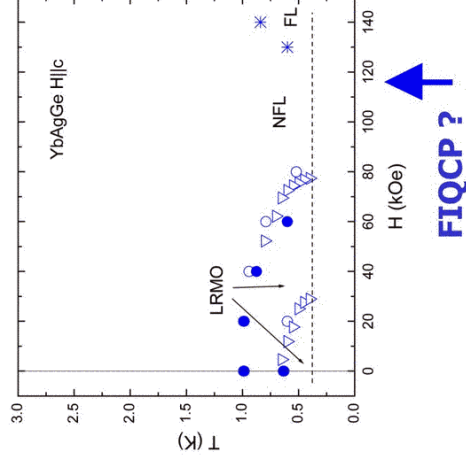
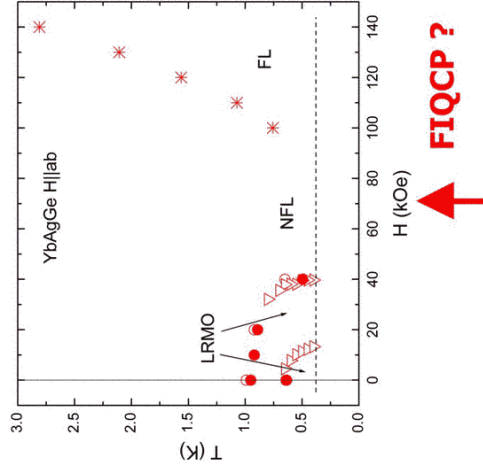


High fields:
 $\rho = \rho_0 + AT^2$:
FL - like

Intermediate fields:
 $\rho = \rho_0 + BT$:
NFL



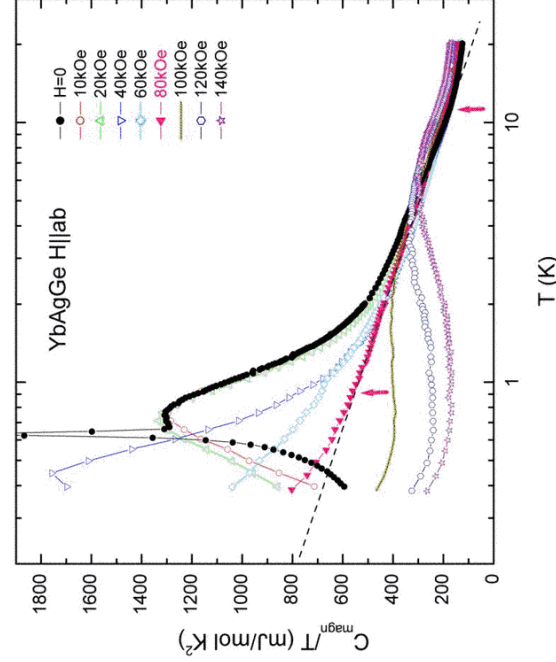
YbAgGe – phase diagrams



2 gram single crystal for scattering from Yuri Janssen

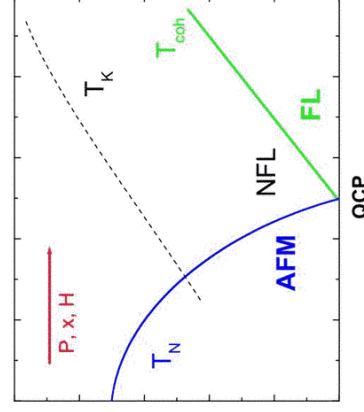
- (i) Tuning via simple and clean knob – H (not P or x)
- (ii) Only second stoichiometric Yb- compound to show this
- (iii) Unlike YbRh₂Si₂ crystals can be BIG

YbAgGe – heat capacity in applied field



H = 80 kOe: $C_{\text{magn}}/T \propto -\ln T$ for over a decade in temperature

$C_{\text{magn}}/T = \gamma'_0 \ln(T_0/T): \gamma'_0 \approx 144 \text{ mJ/mol K}^2; T_0 \approx 41 \text{ K}$

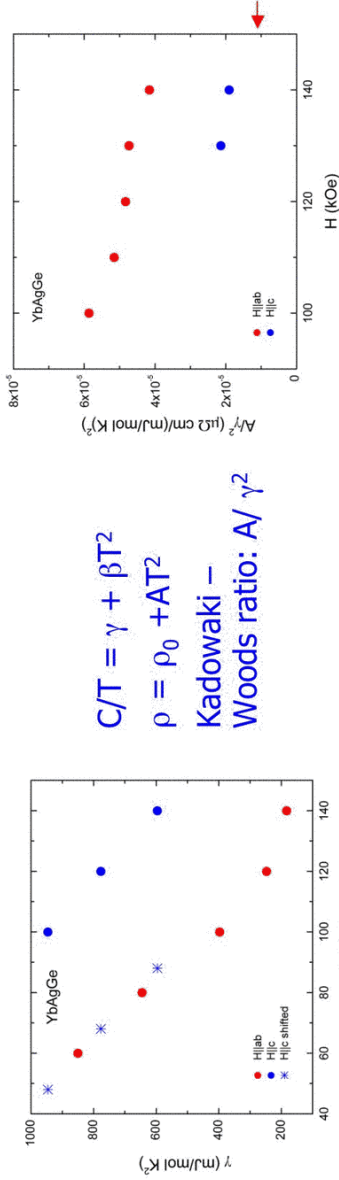


Also: scaling of the specific heat:
 $[C(H)-C(H=0)] \text{ vs. } H/T^\beta,$
 $\beta = 1.15$

(observed in a number of materials with NFL properties)

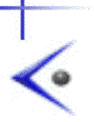
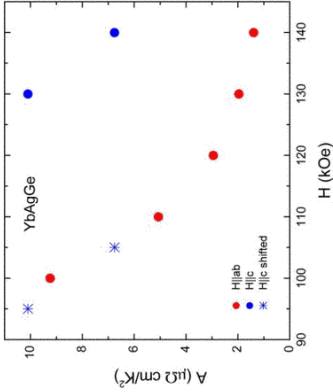
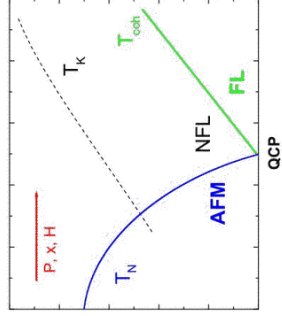


YbAgGe: resistivity and heat capacity coefficients



$C/T = \gamma + \beta T^2$
 $\rho = \rho_0 + AT^2$
 Kadowaki – Woods ratio: A/γ^2

Higher KW ratio close to magnetic instability – Takimoto & Moriya, SSC 99 (1996) 457
Constant – in local critical regime



Hall effect at QCP

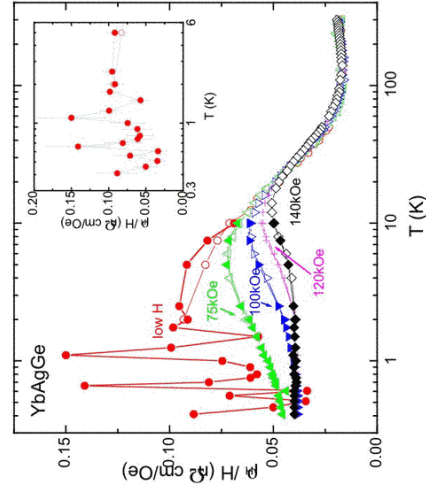
P.Coleman et al., JPCM 13 (2001) R723

- SDW
- breakdown of composite HF

Hall effect as a test:

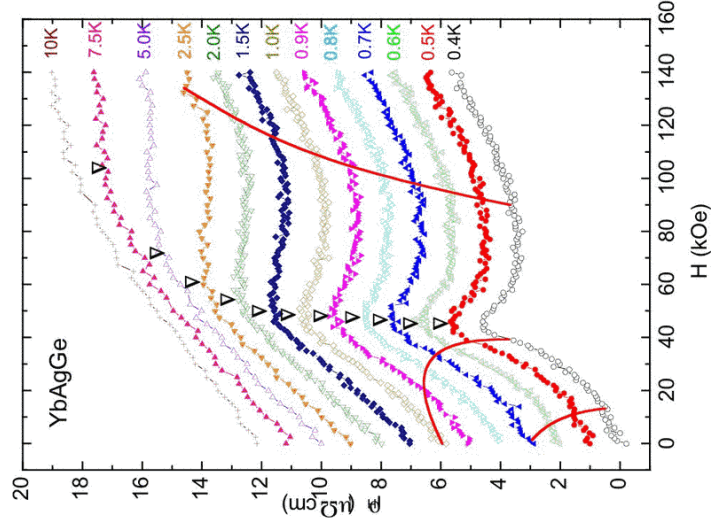
Mechanism	R_H
S. D. W.	
Breakdown of composite Fermions	

YbAgGe – Hall effect (H||ab)

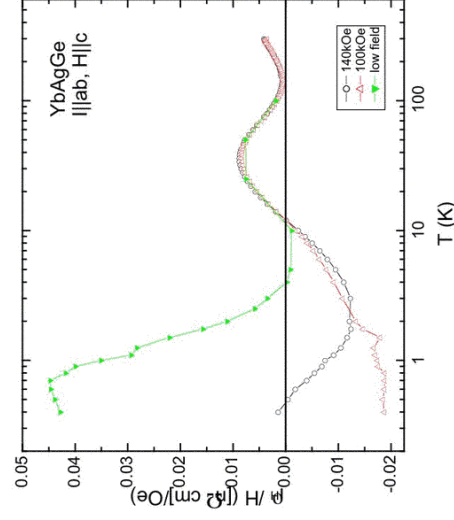


New line on the phase diagram?

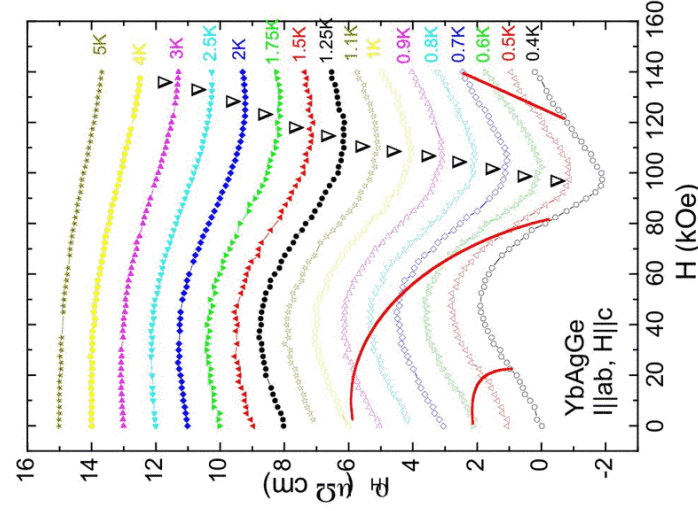
SLB et al, cond-mat/0406435



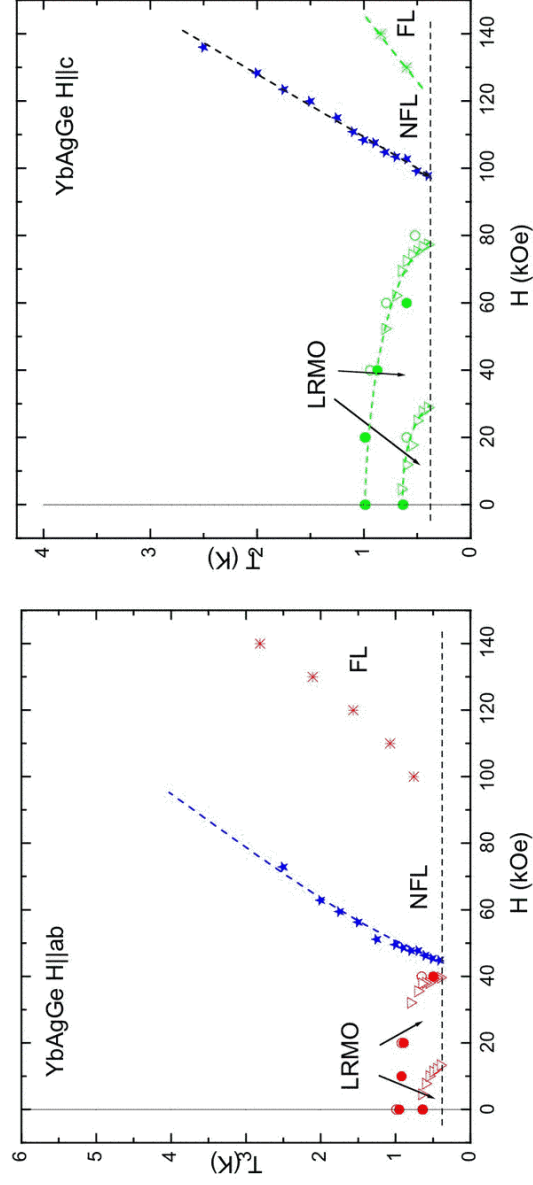
YbAgGe – Hall effect (H||c)



Similar to H||ab



YbAgGe – “revised” phase diagrams

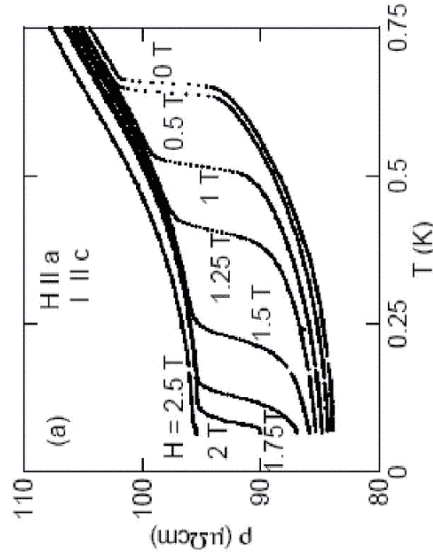


For both field orientations $\rho_H(H)$ define a new line.

From $\rho_H(H)$ no unambiguous choice between the two QCP models.

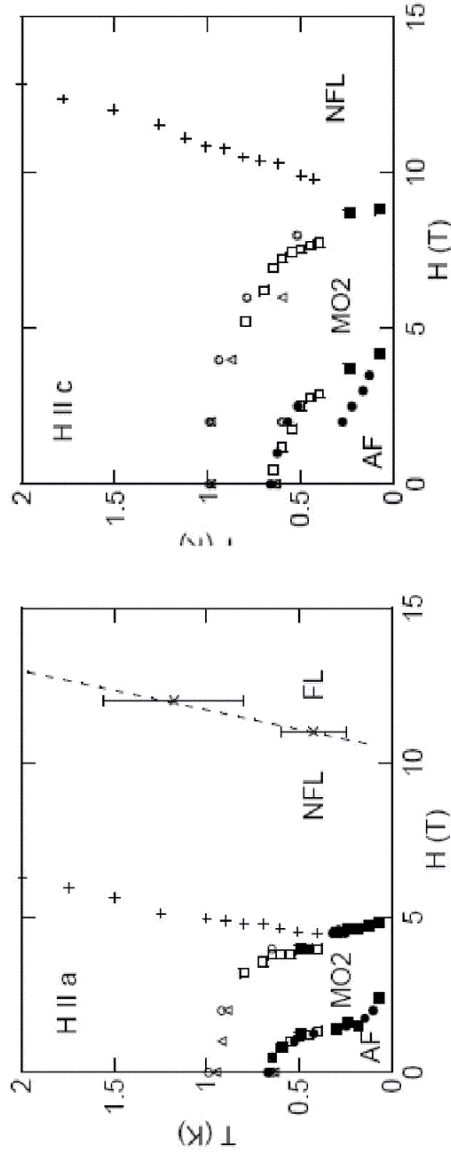
Possible FIQCP in YbAgGe – next steps

- Lower temperatures
- Neutron scattering measurements



Philipp Niklowitz, Jacques Flouquet
(CEA/Grenoble)

YbAgGe H-T Phase diagrams



Extended temperature range data from Philipp Nicklowitz et al., CEA Grenoble. These data further support identification of field induced QCP.



Possible FIQCP in YbAgGe – next steps

Other techniques:

NEUTRON SCATTERING:

- (i) Find and confirm ordering (partially done) and fully determine ordered structure (ongoing).
- (ii) Look at inelastic scattering near QCP (ongoing with several runs scheduled for the first quarter of '05)

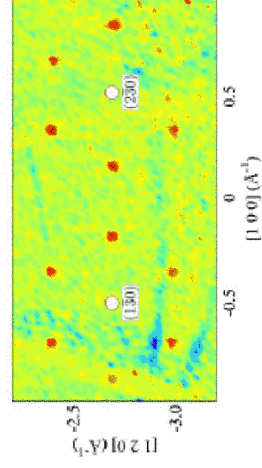


Figure 2. Color map of the low- T magnetic scattering in YbAgGe, taken as the difference between data at $T = 0.32$ and 2.0 K, in the (hk) scattering plane for $l = 1/3$. The six-fold symmetry of the magnetic satellites characterized by a propagation vector of $k=(1/3,0,1/3)$ is easily seen.

Below 0.6 K a $(1/3,0,1/3)$ wave vector evolves.

Björn Fåk, Desmond McMorrow, et al.

JPCM 17 (2005) 301



YbAgGe – Stiochiometric FIQCP compound

- Resistivity: decrease of $T_{\text{magn}} \Rightarrow$ linear LT resistivity \Rightarrow recovery of T^2 (FL) behavior
- Heat capacity: decrease of $T_{\text{magn}} \Rightarrow C_{\text{magn}}/T \propto -\ln T \Rightarrow$ recovery of FL behavior. Scaling of $[C(H)-C(H=0)]$ vs. H/T^β
- Anomaly in Hall resistivity data very clear and apparently associated with FIQCP
- FIQCP in accessible fields ($\leq 11T$) associated with a $H = 0$ T_N that is also very accessible.
- One of the few **stiochiometric** compounds possibly showing FIQCP
- Effects are anisotropic



Conclusions:

- Yb-based heavy fermions offer fertile ground for QCP research
- They allow to address “key” question of how can correlated electron state evolve out of local moment. One can be a voyeur and watch how it happens.
- Few properties are curious and entertaining (for some).
- Potentially can shed light on few open questions in HF physics (if samples and “knobs” are under control).
- Can we find a few more so as to identify unifying trends?



Group: Novel Materials and Ground States

Two permanent members:

<http://cmp.ameslab.gov/personnel/canfield/>

Paul C. Canfield and Sergey L. Bud'ko

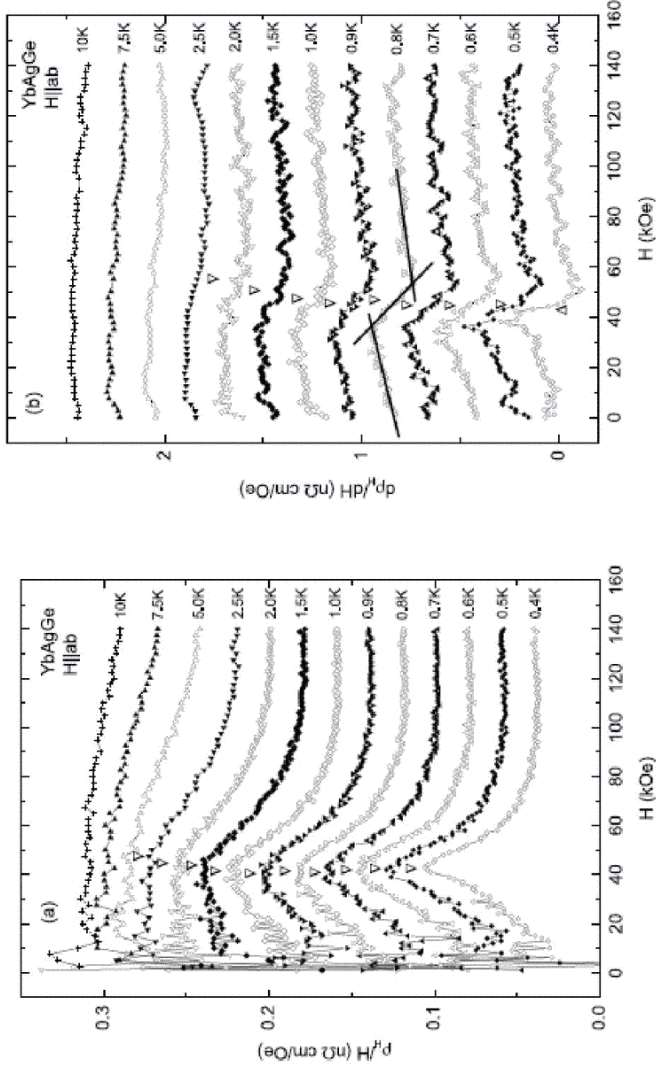
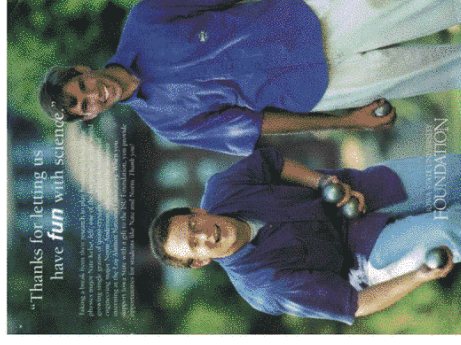
in a steady state:

- 2-3 post-docs / visiting scientists
- 2-4 graduate students
- 1-3 (hourly) undergraduates

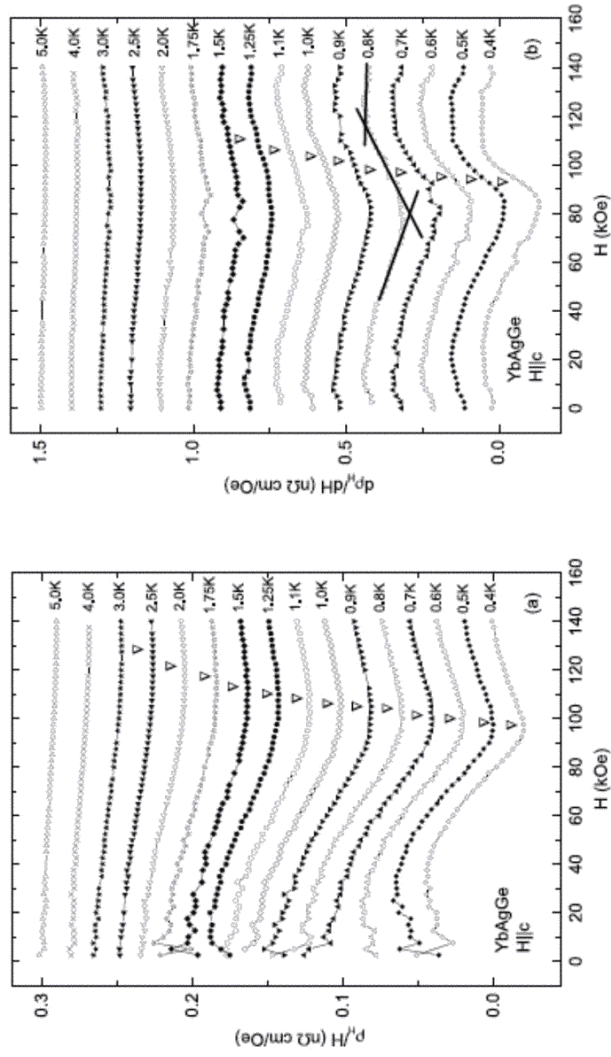
Toys:

- Furnaces, arc-melter
- Powder diffractometer
- 2_ QD MPMS magnetometers
- 1_ QD PPMS systems (with a few widgets and gadgets)
- Polishers, wire & diamond saws, press, etc.

Easy access to Ames Lab resources



➤ S. L. Bud'ko et al., PRB 71 (2005) xxxx. (cond-mat./0406435)



➤ S. L. Bud'ko et al., PRB 71 (2005) xxxx. (cond-mat./0406435)

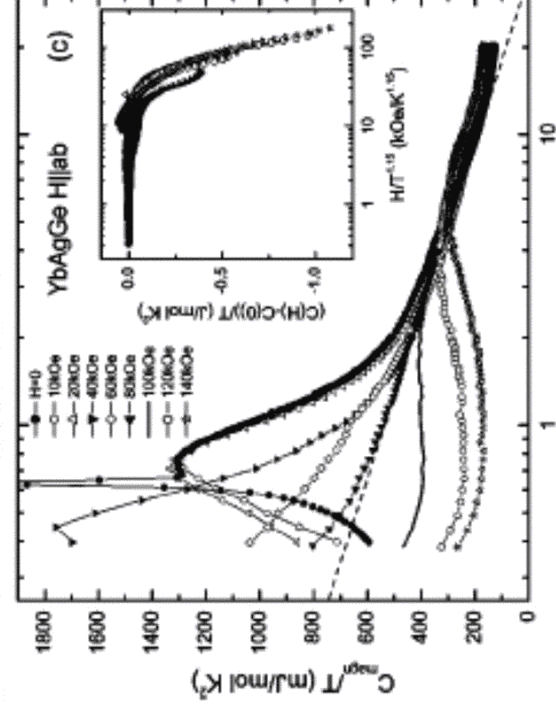


FIG. 5. (a) Low-temperature part of the heat-capacity curves for YbAgGe taken at different applied fields $H\parallel ab$, arrows indicate peaks associated with magnetic ordering; (b) low-temperature part of C_p vs T curves; (c) *semi-log* plot of the magnetic part [$C_p^{magn} = C_p(\text{YbAgGe}) - C_p(\text{LuAgGe})$] of the heat capacity, C_p^{magn}/T vs T , for different applied magnetic fields, dashed line is a guide to the eye, it delineates linear region of the $H = 80$ kOe curve; inset: *semi-log* plot of $[C(H) - C(H=0)]/T$ vs $H/T^{1.15}$ ($T \geq 0.8$ K), note approximate scaling of the data for $H \geq 60$ kOe.

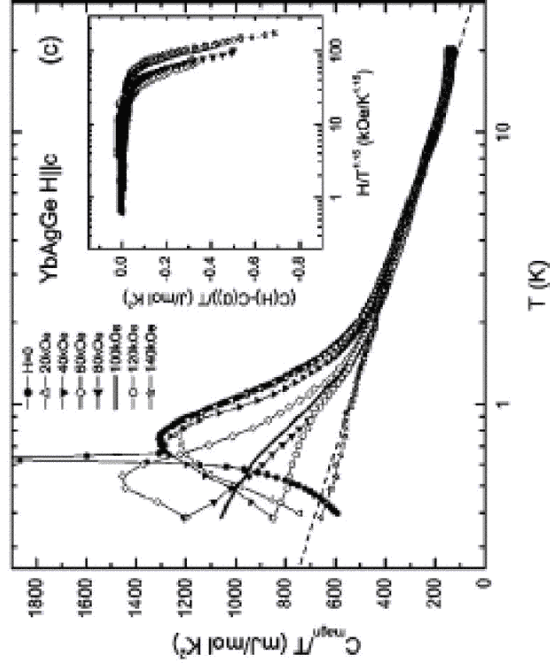


FIG. 8. (a) Low-temperature part of the heat-capacity curves for YbAgGe taken at different applied fields $H\parallel c$, arrows indicate peaks associated with magnetic ordering; (b) low-temperature part of C_p vs T^3 curves; (c) *semi-log* plot of the magnetic part [$C_{\text{mag}}^{\text{low}} = C_p(\text{YbAgGe}) - C_p(\text{LuAgGe})$] of the heat capacity, $C_{\text{mag}}^{\text{low}}/T$ vs T , for different applied magnetic fields, dashed line is a guide to the eye, it delineates linear region of the $H = 140$ kOe curve; inset: *semi-log* plot of $[C(H) - C(H=0)]/T$ vs $H/T^{1.15}$ ($T \geq 0.8$ K), note approximate scaling of the data for $H \geq 100$ kOe.

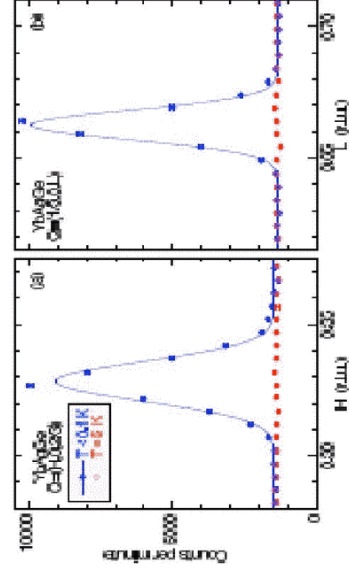


Figure 9. Scans at zero energy transfer along the (a) h and (b) l direction of the $Q=(1/3,0,2/3)$ magnetic Bragg peak of YbAgGe measured on IN14 using $k_f = 1.3 \text{ \AA}^{-1}$. Closed and open circles correspond to temperatures of 0.1 and 5.0 K, respectively. The lines are Gaussian fits.

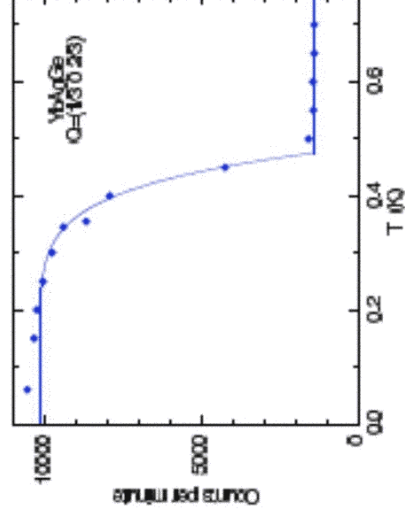


Figure 4. Temperature dependence of the magnetic Bragg peak intensity at $Q=(1/3, 0, 2/3)$ of YbAgGe measured on IN14 using $k_f = 1.3 \text{ \AA}^{-1}$. The line is a guide to the eye.

attering study of YbAgGe

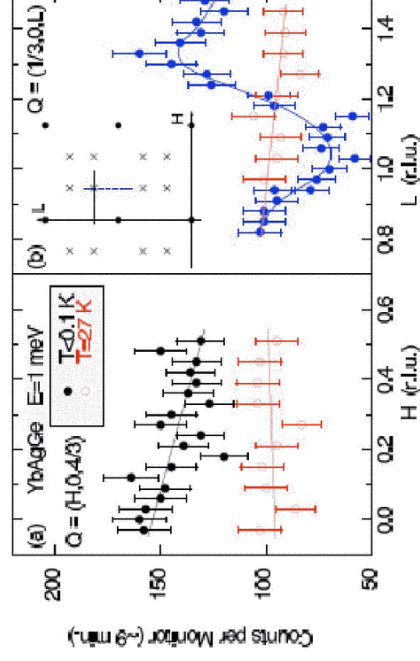


Figure 6. Scans in wave vector Q along the (a) h and (b) l direction of the spin-fluctuation scattering at an energy transfer of $E = 1 \text{ meV}$, measured on IN14 using $k_f = 1.30 \text{ \AA}^{-1}$. Closed and open circles correspond to $T < 0.1$ and $T = 27 \text{ K}$, respectively. The lines are guides to the eye. The inset shows the scan directions in the $(h0l)$ plane.

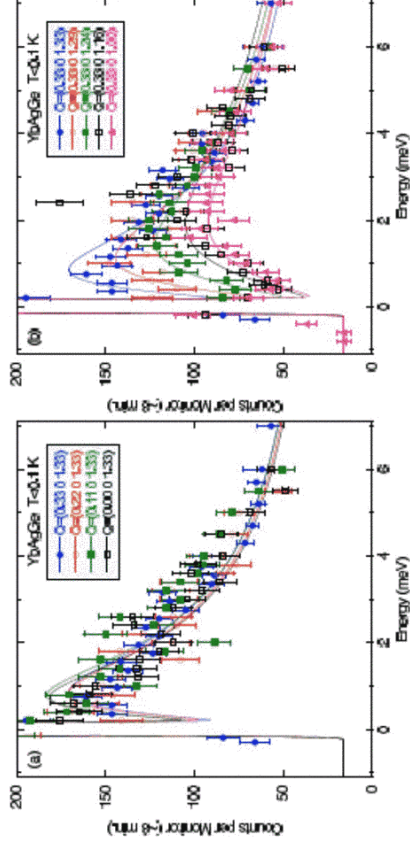


Figure 7. Energy scans of the quasielastic magnetic scattering at low temperatures, $T < 0.1$ K, for different q values along the (a) h and (b) l direction, measured on IN14 using $k_f = 1.30 \text{ \AA}^{-1}$. The lines are fits to a quasielastic Lorentzian, Eqs. (1-2), plus a Gaussian describing the elastic scattering.

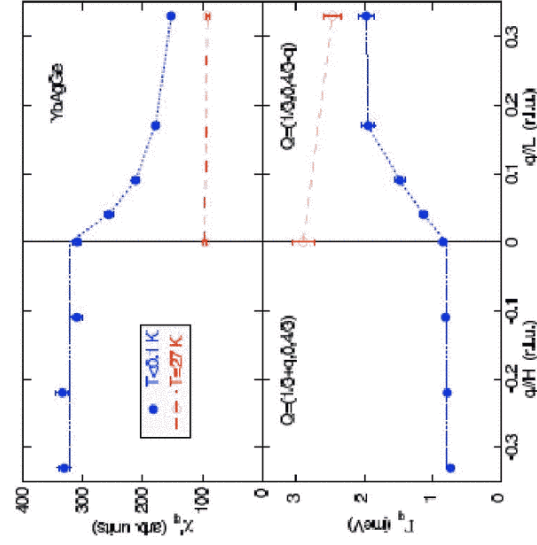


Figure 8. Wave vector dependence of the static susceptibility χ_q^{static} and the characteristic energy Γ_q of the quasielastic magnetic scattering along the h (left part) and l (right part) direction at $T < 0.1$ K (closed circles) and $T = 27$ K (open circles). The lines are guides to the eye.

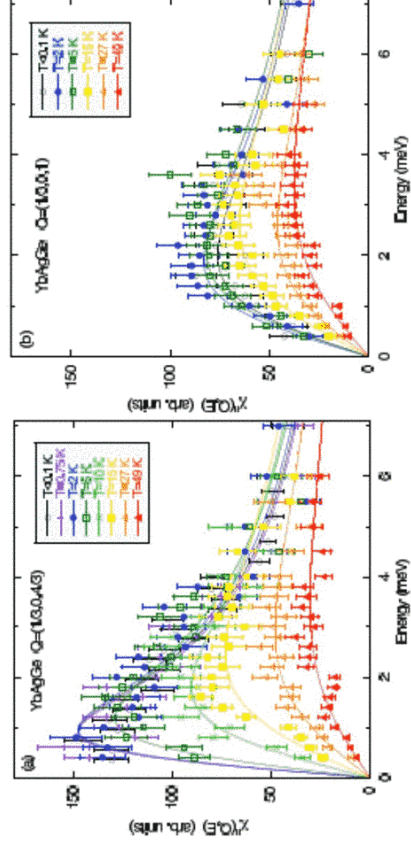


Figure 9. Dynamic magnetic susceptibility for different temperatures at (a) the AFM zone center $Q=(1/3, 0, 4/3)$ and (b) the AFM zone boundary $Q=(1/3, 0, 1)$, measured on IN14 using $k_f = 1.30 \text{ \AA}^{-1}$. The lines are fits to a quasielastic Lorentzian, Eq. (2).

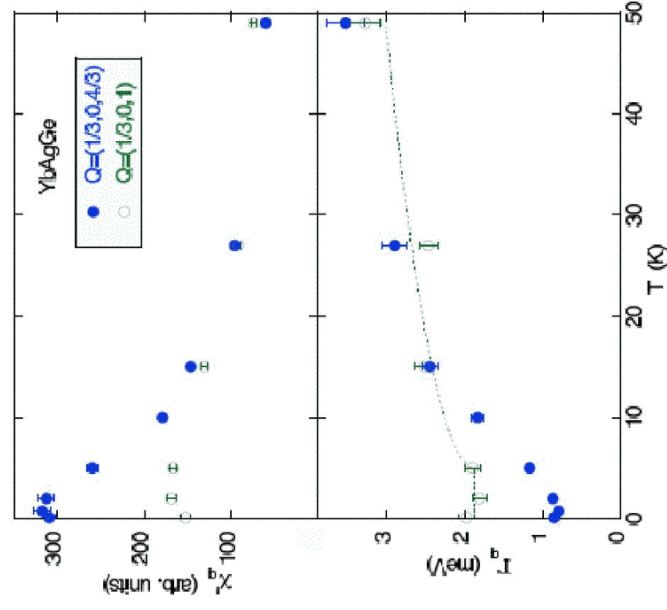


Figure 10. Temperature dependence of the static susceptibility $\chi''_q(T)$ and the characteristic energy $\Gamma_q(T)$ of the quasielastic magnetic scattering at the AFM zone center $Q=(1/3, 0, 4/3)$ (solid circles) and at the AFM zone boundary $Q=(1/3, 0, 1)$ (open circles). The dashed line shows a fit of Eq. (3) to the zone boundary energy Γ_0 .

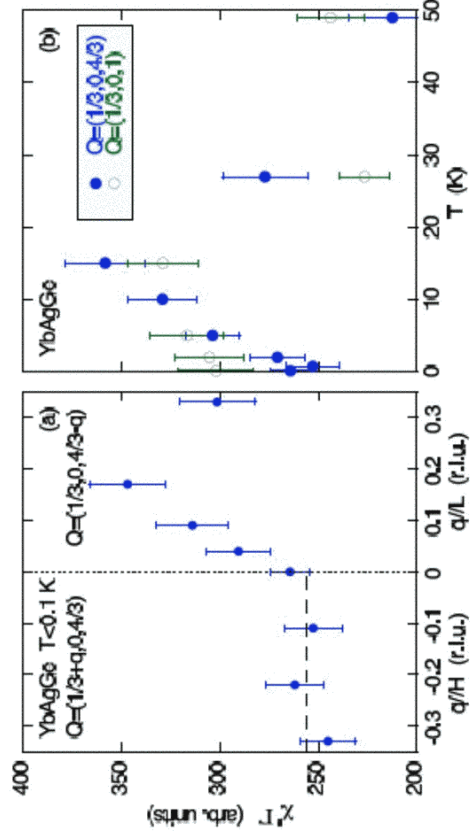


Figure 11. The product $\chi_q(T)$ of the static susceptibility $\chi_q(T)$ and the characteristic energy $\Gamma_q(T)$ of the quasielastic magnetic scattering. (a) $\chi_q(T)$ as a function of q along h (left part) and l (right part). (b) $\chi_q(T)$ as a function of temperature for q at the antiferromagnetic zone center and at the zone boundary.

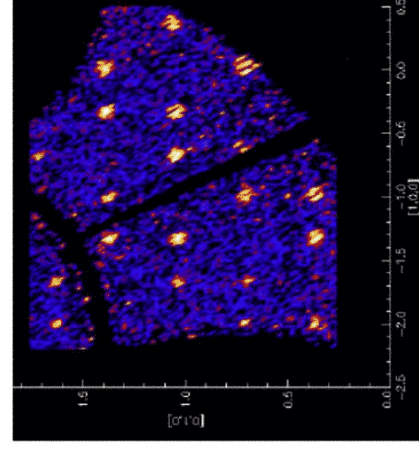


Figure 1: (hk) scattering plane of YbAgGe. Shown is the difference in intensity between $T = 0.32$ and 2.0 K.